

Calorimetric Studies of the Kinetic Unfreezing of Molecular Motions in Hydrated Lysozyme, Hemoglobin, and Myoglobin

Günter Sartor,* Erwin Mayer,* and G. P. Johari†

*Institut für Allgemeine, Anorganische und Theoretische Chemie, Universität Innsbruck, Innsbruck, Austria, and †Department of Materials Science and Engineering, McMaster University, Hamilton, Ontario, Canada

ABSTRACT Differential scanning calorimetric (DSC) studies of the glassy states of as-received and hydrated lysozyme, hemoglobin, and myoglobin powders, with water contents of ≤ 0.25 , ≤ 0.30 , and ≤ 0.29 g/g of protein, show that their heat capacity slowly increases with increasing temperature, without showing an abrupt increase characteristic of glass→liquid transition. Annealing (also referred to as physical aging) of the hydrated proteins causes their DSC scans to show an endothermic region, similar to an overshoot, immediately above the annealing temperature. This annealing effect appears at all temperatures between ~ 150 and 300 K. The area under these peaks increases with increasing annealing time at a fixed temperature. The effects are attributed to the presence of a large number of local structures in which macromolecular segments diffuse at different time scales over a broad range. The lowest time scale corresponds to the $>N-H$ and $-O-H$ group motions which become kinetically unfrozen at ~ 150 – 170 K on heating at a rate of 30 K min^{-1} and which have a relaxation time of 5 – 10 s in this temperature range. The annealing effects confirm that the individual glass transition of the relaxing local regions is spread over a temperature range up to the denaturation temperature region of the proteins. The interpretation is supported by simulation of DSC scans in which the distribution of relaxation times is assumed to be exceptionally broad and in which annealing done at several temperatures over a wide range produces endothermic effects (or regions of DSC scans) qualitatively similar to those observed for the hydrated proteins.

INTRODUCTION

In hydrated proteins a fraction of water of up to ~ 0.3 – 0.4 (g water)/(g protein) remains mobile down to very low temperatures and does not crystallize even during long periods, independent of the rate of cooling or heating (for reviews see Kuntz and Kauzmann, 1974; Cooke and Kuntz, 1974; Rupley and Careri, 1991). Hydrated water above this hydration range crystallizes on slow cooling but can be vitrified with increasing rates of cooling. We recently reported a study by differential scanning calorimetry (DSC) on the vitrification and crystallization characteristics of freezable water in hydrated methemoglobin, of between ~ 0.4 – 0.7 (g water)/(g protein), which can be vitrified but crystallizes on heating (Sartor et al., 1992). One of the conclusions from this study, and of a similar study of water imbibed in the pores of a synthetic hydrogel (Hofer et al., 1990), was that the DSC scans of the sample in which water had crystallized were featureless and qualitatively similar, up to the temperature at which ice melts, to ones in which the sample contained only unfreezable water. Here we report a DSC study of hydrated met-hemoglobin (MetHb), metmyoglobin (MetMb), and lysozyme powders which have been hydrated only up to ~ 0.3 (g water)/(g protein). As already indicated, this corresponds to the hydration range at which water does not crystallize, and complications due to formation of ice on cooling are thus

avoided. We interpret the calorimetric behavior on annealing (also referred to as physical aging) in terms of a broad range of relaxation times over which the relaxation of local regions in its bulk structure occurs. We support our conclusions by simulating the calorimetric behavior and the annealing effects on it, and by comparing it with the calorimetric behavior of a synthetic polymer in which relaxation time distribution is broad. The study is significant in recognizing the local segmental motions of the hydrated hemoglobin, myoglobin, and lysozyme macromolecule that occur over a certain time scale at a given temperature.

Increasingly rapid dynamics of hydrated proteins at ~ 200 K has been observed by various techniques and attributed to a “glass-like” transition (Morozov and Gevorkian, 1985; Frauenfelder and Gratton, 1986; Parak, 1986; Iben et al., 1989; Doster et al., 1986, 1989, 1990, 1991; Goldanskii and Krupyanskii, 1989; Rupley and Careri, 1991; Srajer et al., 1991; Champion, 1992; Pethig, 1992; Pissis et al., 1992). In particular, DSC measurements of myoglobin crystals and hydrated powders have been made, and an increase in heat capacity observed at ~ 220 K has been attributed to glass→liquid transition of water (Doster et al., 1986). This temperature of ~ 220 K is much higher than the onset temperature of the glass transition (or T_g) of 136 K for pure bulk water (Johari et al., 1987; Hallbrucker et al., 1989), or ≈ 162 – 170 K for vitrified and freezable water in hydrated MetHb (Sartor et al., 1992) or in a synthetic hydrogel (Hofer et al., 1990). This discrepancy needs to be examined. Furthermore, calorimetry shows that annealing from ~ 150 K up to the temperature region of denaturation has a substantial calorimetric effect which may be confused with glass transition and its onset temperature. These effects are also described in

Received for publication 26 July 1993 and in final form 12 October 1993.

Address reprint requests to Dr. E. Mayer, Institut für Allgemeine, Anorganische und Theoretische Chemie, Universität Innsbruck, A-6020 Innsbruck, Innrain 52 a Austria.

© 1994 by the Biophysical Society

0006-3495/94/01/249/10 \$2.00

this study, and it is shown that the dynamics of protein molecules are determined by a very broad distribution of local relaxation times in its different segmental regions.

MATERIALS AND METHODS

Hemoglobin from human blood (No. H 7379) and myoglobin (No. M 0630) were obtained from Sigma Chemical Co. (St. Louis, MO). Both were characterized in aqueous solution (phosphate buffered at pH 6.8) by their ultraviolet (UV)-visible spectra to be MetHb (Waterman, 1978) and MetMb (Rothgeb and Gurd, 1978) and were used as received. Lysozyme (No. L 6876) was also obtained from Sigma. For Fig. 6, methemoglobin from bovine blood (Fluka, No. 51290) was used.

The proteins were hydrated by keeping them over saturated salt solutions at a constant temperature for several weeks, following Poole and Finney's (1986) description of preparation of solid-phase low hydration samples. Water content of the as-received proteins, determined by heating to 378 K, was 0.10 (g water)/(g protein) for hemoglobin and lysozyme, and 0.08 (g water)/(g protein) for myoglobin. Poole and Finney (1986) pointed out that "this method of drying may leave behind a few strongly bound waters, and hence an uncertain, though relatively small, zero error," and mentioned that dried lysozyme powders still contained ~ 0.01 (g water)/(g lysozyme). For simplicity we have neglected this small amount of water and in the following sections will consider the proteins as "dry" after they have been heated at 378 K to constant weight, transferred to a desiccator and weighed. Final water content of the hydrated proteins was determined by weighing to ± 0.01 mg, taking into account the water content of the as-received proteins. The hydrated proteins were quickly crimp-sealed into aluminum pans and weighed. The accuracy of the given hydration values is estimated to be ± 0.02 (g water)/(g protein).

A Perkin-Elmer differential scanning calorimeter (DSC), model DSC-4, with TADS computer-assisted data acquisition, was used for all studies. Curvature of the traces was eliminated with the SAZ function which subtracts the baseline obtained with empty sample pans during scanning. X-Y data were transferred via serial interface from TADS to a PC and manipulated by SpectraCalc. Only crimp-sealed aluminum pans were used to avoid evaporation losses and to obtain cooling rates of up to ~ 150 K min^{-1} in the DSC instrument. The weights of the samples were between 7.60 and 28.89 mg. Further experimental details on DSC are given by Sartor et al. (1992), Hofer et al. (1990), and Hallbrucker et al. (1989).

After several of the experiments, the UV-visible spectra of the proteins dissolved in phosphate buffer (pH 6.8) were recorded again and found to be indistinguishable from those of the proteins before exposure to the cooling/heating cycles. This is evidence that no irreversible denaturation had occurred.

RESULTS

The DSC scans of as-received and hydrated protein powders obtained by cooling from 298 K to 103 K at ~ 150 K min^{-1} and thereafter heating at 30 K min^{-1} are shown in Fig. 1. Curves 1 and 2 show scans of lysozyme, containing 0.10 (as-received) and 0.25 (g water)/(g lysozyme). The corresponding scans of as-received (0.10) and 0.30 (g water)/(g MetHb) have been included as curves 3 and 4, and of as-received (0.08) and 0.29 (g water)/(g MetMb) as curves 5 and 6 to show the similarity between their respective features. For all proteins, the endothermic effect or equivalently the heat capacity, C_p , of the hydrated sample increases more rapidly with temperature than the endothermic effect of the as-received sample of low water content.

For annealing studies, the samples were cooled from 298 K to 103 K at ~ 150 K min^{-1} , heated to the annealing tem-

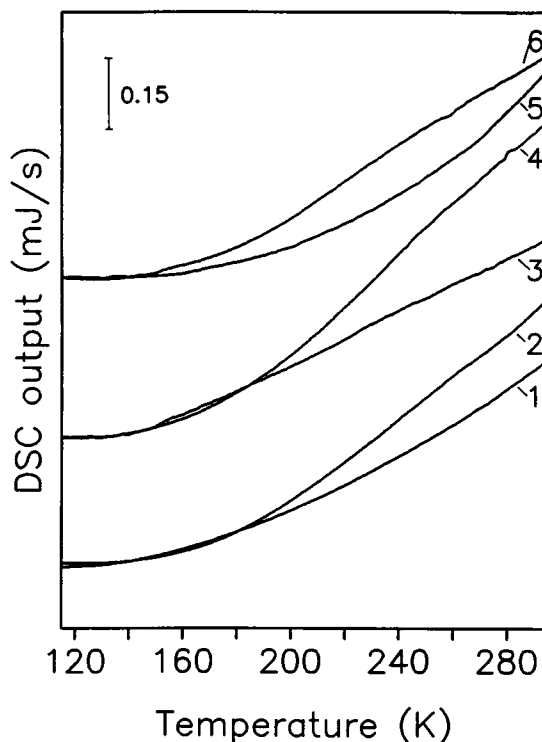


FIGURE 1 The DSC scans of as-received lysozyme containing 0.10 (g water)/(g lysozyme) (curve 1) and hydrated lysozyme containing 0.25 (g water)/(g lysozyme) (curve 2) obtained during heating at 30 K min^{-1} . The two curves are drawn overlapped and the area above the curve of the as-received protein at $T > \sim 170$ K indicates the configurational contribution to C_p , which the atomic and segmental motions of the protein molecules make, as these motions become kinetically unfrozen (they do not represent absolute C_p of the proteins). Curves 3 and 4 are the corresponding DSC scans for as-received MetHb and hydrated MetHb containing 0.10 and 0.30 (g water)/(g MetHb), respectively. Curves 5 and 6 are the corresponding curves for as-received MetMb and hydrated MetMb containing 0.08 and 0.29 (g water)/(g MetMb), respectively. The samples were cooled in the instrument from 298 K to 103 K at a rate of ~ 150 K min^{-1} in all cases. The curves are drawn on the same scale and are normalized with respect to the weight of the samples. The bar marks the ordinate scale. In general, for Figs. 1–9, the curves are shifted vertically for clarity. The ordinate scales are for 1 mg sample weight. The temperature axes are not corrected for thermal lag of the instrument.

perature at 30 K min^{-1} and kept for 60 min, cooled to 103 K at 30 K min^{-1} , and finally heated at 30 K min^{-1} to 298 K and the DSC scan obtained. In Fig. 2 we show the effect of annealing a sample of hydrated MetHb containing 0.30 (g water)/(g MetHb) at 198 K in the form of DSC subtraction curves and compare it with those of the original DSC curves. Curves 1 and 2 are the scans of the unannealed sample recorded immediately one after the other, curve 3 is the scan of the same sample which had in addition been annealed at 198 K for 60 min before its heating (marked by arrow). The effect of annealing is seen in curve 3 in the form of a weak endothermic feature. This endothermic feature is seen more clearly by subtracting curve 2 from curve 3 and is now shown as curve 5 on a twofold enlarged scale. An estimate for baseline stability was obtained by curve 4 which was obtained by subtracting curve 1 from curve 2 and which is shown on the

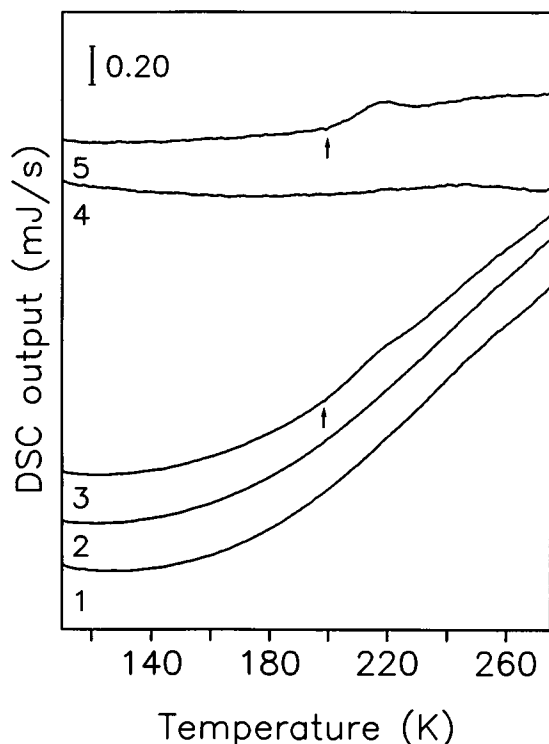


FIGURE 2 The effect of annealing at 198 K shown in DSC scans of a hydrated methemoglobin sample containing 0.30 (g water)/(g MetHb) and in DSC subtraction curves. Curves 1 and 2 are for the unannealed sample recorded immediately one after the other; curve 3 is for the same sample but annealed in addition at 198 K for 60 min. Curve 4 was obtained by subtracting curve 1 from curve 2, and curve 5 was obtained by subtracting curve 2 from curve 3. The annealing temperature is indicated by arrows. The sample was cooled from 298 K to 103 K at ~ 150 K min^{-1} and reheated at 30 K min^{-1} . Curves 1–3 are drawn on the same scale (indicated by the bar for 1 mg weight); curves 4 and 5 are drawn on a twofold enlarged scale.

same scale as curve 5. This curve lacks the endothermic peak and shows only a slight deviation from the horizontal which can be taken as indicator for baseline stability. The endothermic feature in curve 5 has a signal-to-noise ratio of ~ 14 which can be increased further by smoothing if necessary. This set of curves clearly demonstrates that the quality of our DSC instrument is sufficient for this type of study. In the following we show only the original DSC curves.

Fig. 3 shows as curve 1 the DSC scans for the unannealed sample of lysozyme containing 0.23 (g water)/(g lysozyme), and as curves 2 to 5 the scans of the same sample but annealed for 60 min at 198 K (curve 2), 233 K (curve 3), 253 K (curve 4), and 278 K (curve 5). For curve 5 the sample was heated to 323 K. The annealing temperatures are marked by arrows. The scans show, after annealing, a slight endothermic increase beginning near the annealing temperature, which is marked for clarity by the shaded area in curves 2 to 5.

Figs. 4 and 5 show similar scans for hydrated MetHb (Fig. 4) containing 0.30 (g water)/(g MetHb) and hydrated MetMb (Fig. 5) containing 0.28 (g water)/(g MetMb), with curve 1 for the unannealed sample and curves 2 to 5 for the same sample but annealed at 198 K (curve 2), 238 K (curve 3), 258 K (curve 4), and 278 K (curve 5). Here the scans also show

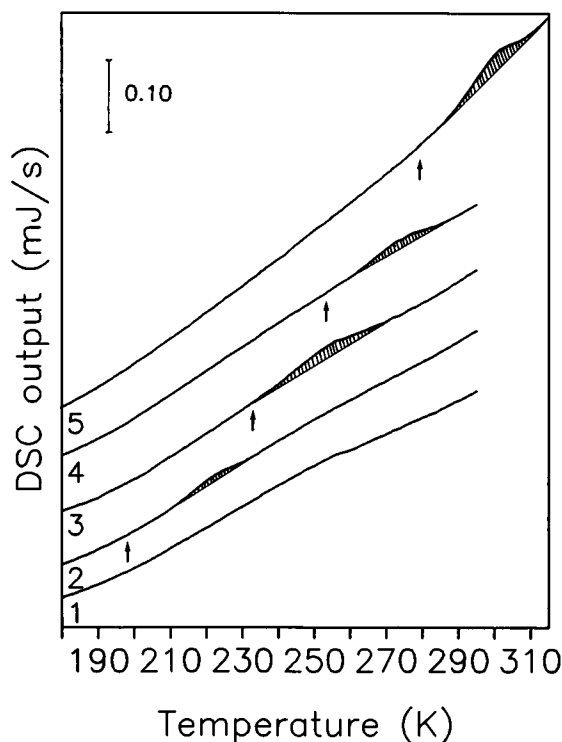


FIGURE 3 The DSC scans of hydrated lysozyme containing 0.25 (g water)/(g lysozyme) obtained after annealing at various temperatures for 60 min. Curve 2 is for a state obtained after annealing at 198 K, curve 3 for that at 233 K, curve 4 for that at 253 K, and curve 5 for that at 278 K. Curve 1 is the scan of the unannealed sample and is shown for comparison. The annealing temperatures are indicated by arrows, and the endothermic features by the shaded regions. For curves 2–5 the sample was first cooled from 298 K to 103 K at ~ 150 K min^{-1} , heated to the annealing temperature at 30 K min^{-1} , kept at the annealing temperature for 60 min, cooled to 103 K at 30 K min^{-1} , and finally reheated to 298 K (or 323 K for curve 5) at 30 K min^{-1} when its DSC scan was taken. The curves are drawn on the same scale.

a slight endothermic increase, indicated by the shaded area which begins near the annealing temperature as marked in curves 2 to 5.

The effects of annealing at temperatures between 150 K and 198 K were also investigated, and the endothermic features became increasingly weaker with decreasing temperature (not shown). Annealing above 278 K, up to the temperature of denaturation, resulted in features similar to curves 5 in Figs. 3 to 5.

Fig. 6 shows the effect of varying the annealing time at a fixed temperature of 198 K for a sample of hydrated MetHb containing 0.24 (g water)/(g MetHb). The DSC scans 1 to 6 were recorded on reheating from 103 K to 298 K at a rate of 30 K min^{-1} , after annealing for 5, 10, 15, 30, 45, and 60 min, respectively. The area of the endothermic feature and its high temperature range clearly increase with increasing annealing time, but the beginning at low temperature is barely affected by the annealing time. Immediately after scan 6, the experiment was repeated with the same sample and close to identical DSC curves were obtained on reheating for annealing at 198 K from 5 to 60 min. This is an important point and

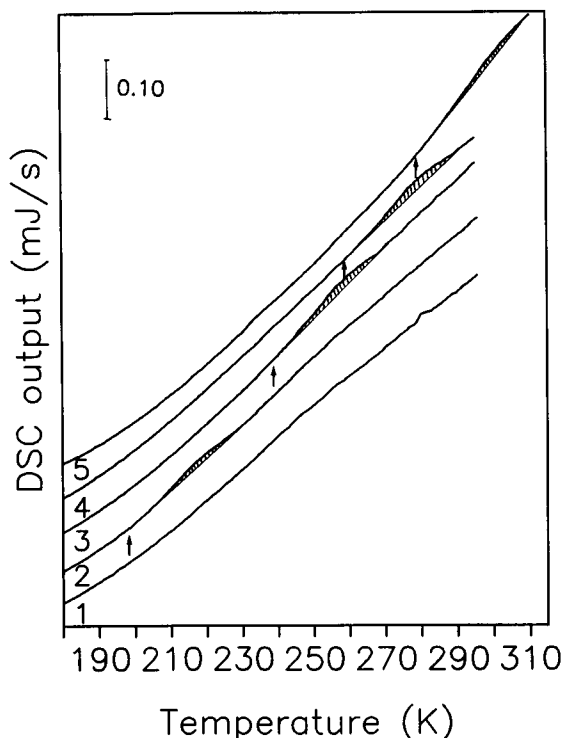


FIGURE 4 The DSC scans of hydrated methemoglobin containing 0.30 (g of water)/(g of MetHb) obtained after annealing at various temperatures for 60 min. Curve 2 is for a state obtained after annealing at 198 K, curve 3 for that at 238 K, curve 4 for that at 258 K, and curve 5 for that at 278 K. Curve 1 is the scan of the unannealed sample and is shown for comparison. The annealing temperatures are indicated by arrows, and the endothermic features by the shaded regions. For curves 2–5 the sample was first cooled from 298 K to 103 K at ~ 150 K min^{-1} , heated to the annealing temperature at 30 K min^{-1} , kept at the annealing temperature for 60 min, cooled to 103 K at 30 K min^{-1} , and finally reheated to 298 K (or 323 K for curve 5) at 30 K min^{-1} and its DSC scan recorded. The curves are drawn on the same scale.

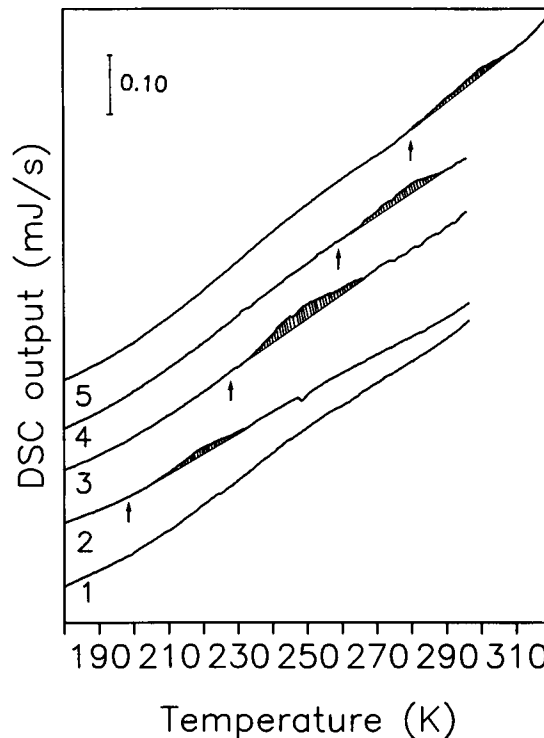


FIGURE 5 The DSC scans of hydrated metmyoglobin containing 0.28 (g water)/(g MetMb) obtained after annealing at various temperatures for 60 min. Curve 2 is for a state obtained after annealing at 198 K, curve 3 is for the state at 238 K, curve 4 is for the state at 258 K, and curve 5 is for the state at 278 K. Curve 1 is the scan of the unannealed sample and is shown for comparison. The annealing temperatures are indicated by arrows, and the endothermic features by the shaded regions. For curves 2–5 the sample was first cooled from 298 K to 103 K at ~ 150 K min^{-1} , heated to the annealing temperature at 30 K min^{-1} , kept at the annealing temperature for 60 min, cooled to 103 K at 30 K min^{-1} , and finally reheated to 298 K (or 323 K for curve 5) at 30 K min^{-1} when its DSC scan was taken. The curves are drawn on the same scale.

proves that the endothermic features are not caused by some irreversible process.

Figs. 7, 8, and 9 show the influence of the water content on the annealing effect. Fig. 7 shows the DSC scans of lysozyme samples containing 0.10 (curve 1), 0.20 (curve 2), and 0.25 (g water)/(g lysozyme) (curve 3), which were annealed at 198 K for 60 min. The endothermic increase was again marked by the shaded area. In curve 1 no endothermic increase is visible but the area increases from curve 2 to curve 3.

Figs. 8 and 9 show the corresponding scans of MetHb samples (Fig. 8) containing 0.10 (curve 1), 0.20 (curve 2), and 0.30 (g water)/(g MetHb) (curve 3), and of MetMb samples (Fig. 9) containing 0.08 (curve 1), 0.20 (curve 2), and 0.28 (g water)/(g MetMb) (curve 3), which were also annealed at 198 K for 60 min. An increase of the shaded area with increasing hydration is obvious.

It is important to note that the endothermic features shown in Figs. 2 to 9 can be observed only when the sample had been annealed before its heating and recording the DSC scan. Samples which were subsequently cooled at various rates and

reheated *without* annealing, did not show these endothermic features. This was tested in particular for a MetHb sample containing 0.24 (g water)/(g MetHb) which, after annealing at 198 K for 60 min, gave on reheating an endothermic feature similar to that shown in Fig. 6 as curve 6. This sample was heated in this experiment to 248 K, cooled either at 5 K min^{-1} or at ~ 150 K min^{-1} and reheated and its DSC scan recorded. Both DSC scans lacked the endothermic feature.

DISCUSSION

Before analyzing the endothermic features seen in the DSC scans on heating, we want to emphasize the following: (i) The features are not due to the melting of ice originating from partial conversion of nonfreezable water into freezable water as a result of annealing. Endothermic features observable between 280 K and 310 K after annealing at 278 K (see Figs. 3–5, curves 5) rule out this possibility. (ii) We believe we can also rule out the possibility that the endotherms are due to annealing-induced crystallization and subsequent melting of some other ordered material, e.g., of some hydrated moiety.

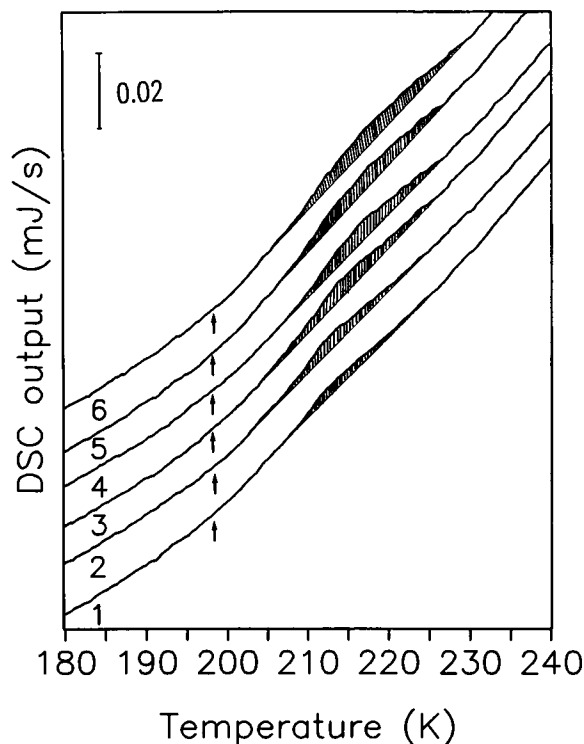


FIGURE 6 The DSC scans of hydrated methemoglobin containing 0.24 (g water)/(g MetHb) obtained after annealing at a fixed temperature of 198 K for various annealing periods. Curves 1–6 were recorded after annealing for, 5, 10, 15, 30, 45, and 60 min, respectively. For each curve the sample was cooled at ~ 150 K min^{-1} , annealed, cooled to 103 K, and thereafter heated at 30 K min^{-1} to 248 K and its DSC scan taken. The annealing temperature is indicated by arrows, and the endothermic feature by the shaded region. The curves are drawn on the same scale.

If partial crystallization was to occur on annealing as it does for nylons (Avramova and Fakirov, 1983), the sample should show an endotherm on reheating, but at a higher temperature than before, because crystallites, if formed, grow and their melting point increases according to the Gibbs-Thomson equation (Wunderlich, 1990). However, we find that increase of the annealing time at a fixed temperature only influences the area of the endothermic feature and its high-temperature end, but not its beginning at low temperature as seen in Fig. 6. In addition, no endotherm can be observed after heating the annealed sample above the temperature of the endothermic feature, slow cooling and subsequent reheating, and recording the DSC scan. (iii) The endothermic features are not due to reversible cold denaturation of the proteins. Endothermic peaks resulting from cold denaturation have been observed (Privalov et al., 1986) and calculated (Franks et al., 1988) for reheating aqueous solutions of myoglobin from subambient temperatures. But, according to Franks and Hatley (1985), cold denaturation is a slow process and even a cooling rate of only ~ 2 K min^{-1} is too fast for internal equilibration of the protein. Because we used cooling rates of 150 K min^{-1} , we are confident that we can rule out this possibility also.

We first discuss the shape of the DSC scans for hydrated proteins and the annealing effects on the scans. For unan-

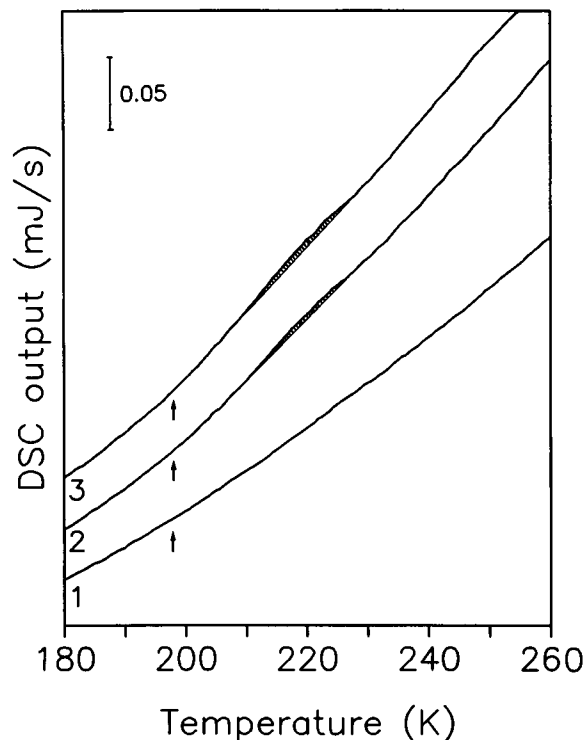


FIGURE 7 The DSC scans of hydrated lysozyme containing various amounts of water obtained after annealing for 60 min at 198 K. Curve 1 is for an as-received sample containing 0.10 (g water)/(g lysozyme), curve 2 for 0.20 (g water)/(g lysozyme), and curve 3 for 0.25 (g water)/(g lysozyme). In all cases the sample was cooled in the instrument from 298 K to 103 K at ~ 150 K min^{-1} , heated to 198 K at 30 K min^{-1} , kept at 198 K for 60 min, cooled to 103 K at 30 K min^{-1} , and finally reheated to 298 K at 30 K min^{-1} when its DSC scan was obtained. The curves are drawn on the same scale and are normalized with respect to the dry weight of the samples.

nealed samples none of the DSC scans in Fig. 1 show a sharp rise in C_p , such as that attributed to the onset of glass transition at T_g . However, the DSC scans of annealed samples do show a change in the slope that seems like the usual onset of glass transition of a substance. But this change in slope should not be taken as T_g of the sample for the obvious reason that this change occurs near the annealing temperature and therefore is observable, as seen in Figs. 3–5, over a range of temperatures from 198 K to 278 K. Although DSC measurements of myoglobin crystals and hydrated powders have been made and the increase in C_p on hydration has been noticed and interpreted in terms of a glasslike transition of water (Doster et al., 1986), such annealing effects as described here from 150 K up to the temperature region of denaturation have not been observed before.

The broad and essentially featureless DSC scan of an unannealed hydrated protein seems to be a result of a broad distribution of relaxation times for atomic and segmental motions of the proteins and of water. At the temperature at which such motions become kinetically unfrozen, a contribution to configurational entropy and C_p appears. This temperature increases with increasing the heating rate. But the temperature range and the magnitude of this effect increases with increasing the annealing time, as can be seen in Fig. 6.

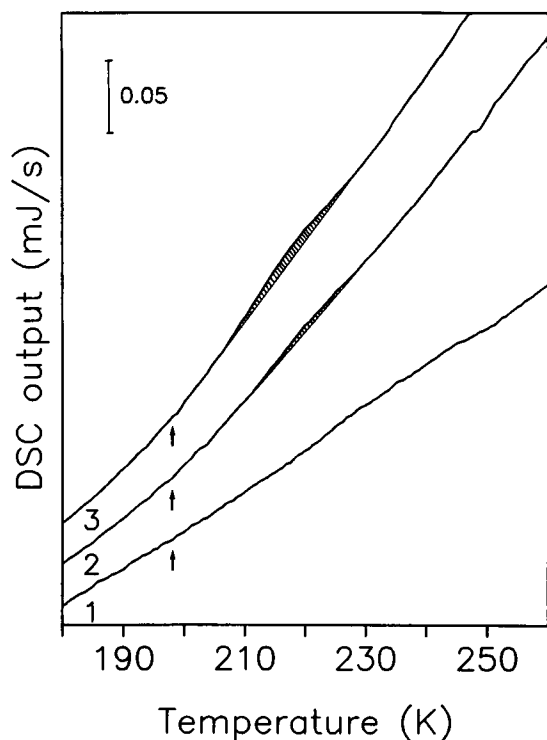


FIGURE 8 The DSC scans of hydrated methemoglobin containing various amounts of water obtained after annealing for 60 min at 198 K. Curve 1 is for an as-received sample containing 0.10 (g water)/(g MetHb), curve 2 for 0.20 (g water)/(g MetHb), and curve 3 for 0.30 (g water)/(g MetHb). The curves are drawn on the same scale and are normalized with respect to the dry weight of the samples. The procedure for annealing is the same as described for lysozyme in Fig. 7.

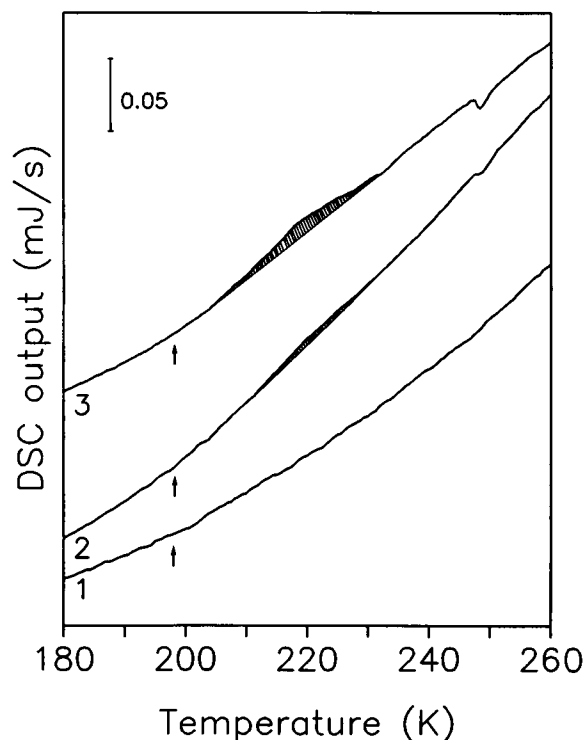


FIGURE 9 The DSC scans of hydrated metmyoglobin containing various amounts of water obtained after annealing for 60 min at 198 K. Curve 1 is for an as-received sample containing 0.08 (g water)/(g MetMb), curve 2 for 0.20 (g water)/(g MetMb), and curve 3 for 0.28 (g water)/(g MetMb). The procedure for annealing is the same as described for lysozyme in Fig. 7. The curves are drawn on the same scale and are normalized with respect to the dry weight of the samples.

Such motions have been inferred from a variety of spectroscopic and other techniques (Morozov and Gevorkian, 1985; Frauenfelder and Gratton, 1986; Parak, 1986; Iben et al., 1989; Doster et al., 1986, 1989, 1990, 1991; Goldanskii and Krupyanskii, 1989; Rupley and Careri, 1991; Srajer et al., 1991; Champion, 1992; Pethig, 1992; Pissis et al., 1992), but were not observed in the same manner as here.

The interpretation of the endothermic regions shown by the shaded areas in Figs. 3 to 5 seems clear to us. As a hydrated protein is annealed at a certain temperature, all modes with molecular relaxation times corresponding to the annealing period become kinetically unfrozen and tend to achieve their respective lower energy state. In this process enthalpy and entropy is released. This is identical with the effect of annealing of a polymer or a glass at a temperature immediately below its T_g . The rate of heating of the sample after annealing causes it to cross the thermodynamic equilibrium curves for all relaxational modes involved in the loss of enthalpy and entropy, and thereafter the glass at $T > T_g$ absorbs heat at a certain rate to approach the equilibrium curve from below, and an endothermic effect (or region in the DSC scan) is observed. The endothermic effect resembles the C_p "overshoot" in the usually observed glass→liquid transition of a glass with a narrow distribution of relaxation times. (Similar observations in the glass transition endotherm

have been referred to as slow enthalpy relaxation by Fransson and Bäckström (1987)). This is a general characteristic of the kinetic sluggishness and the thermodynamic properties. The area under the endothermic feature is a measure of the enthalpy released on annealing. Because annealing at all temperatures between ~ 150 K and the denaturation temperature of the proteins produces an endothermic feature, it follows that molecular or atomic motions in the three hydrated proteins occur with discrete rates for each mode of motion, which become kinetically unfrozen at a certain temperature depending on the preexponential factor and the activation energy for that motion. Alternatively stated, the glass transition in hydrated hemoglobin, myoglobin, and lysozyme does not occur at a single temperature or in a narrow range of temperature but occurs over a broad temperature range that extends from ~ 150 K up to the denaturation temperature. Therefore, no single glass transition temperature can be assigned to the three hydrated proteins, and assignment of a single glass transition temperature in proteins in the sense used for synthetic polymers and molecular substances can be misleading.

In strict physical terms, the relaxation or diffusion time of an atomic or molecular segment has a lower limit which cannot be below the vibrational period of atoms. This limit would be the characteristic diffusion or relaxation time of the

smallest atom, molecule, group, or macromolecules's segment. In hydrated hemoglobin, myoglobin, and lysozyme, this shortest relaxation time would be for the rearrangement of an $>\text{N}-\text{H}$, or of $-\text{O}-\text{H}$ groups covalently or H-bonded to the macromolecules' structure. This means that the three hydrated proteins have a lower temperature limit, or T_{\min} , which corresponds to the temperature at which the fastest motions become unfrozen during the heating at a certain rate. Thus even when the DSC scans are broad as in Fig. 1, there should be a small change in slope beginning at T_{\min} . We are unable to determine this temperature from DSC scans for experimental reasons, and therefore give a range of temperatures for T_{\min} . This is discernible in curves 2, 4, and 6 of Fig. 1 for the three hydrated proteins between ~ 140 and 170 K.

For 30 K min^{-1} heating rate the relaxation time at the onset temperature of glass transition in a DSC scan is ≈ 7 s when the distribution of relaxation times is not taken into consideration (Angell and Torrell, 1983). This time is longer than 7 s when the mode of relaxation has a broad distribution. Although the T_{\min} corresponds to the fastest relaxation process here, the temperature range over which the DSC scan of the hydrated proteins deviates from those of the as-received is as high as ~ 140 – 170 K. It is not certain whether this process itself occurs with a time-dependent rate, as in hierarchically constrained motions, where the effect of kinetic unfreezing of the next (and immediate) slower mode significantly affects the determination of T_{\min} . We conclude that within these uncertainties, the relaxation time at T_{\min} for the fastest mode of motion occurring with a single relaxation time, is between 5 and 10 s. It corresponds to the motion of the shortest group or smallest atom with the lowest energy barrier for hindered rotation.

To obtain independent evidence for our interpretation, it seemed necessary to do a similar study of a synthetic polymer with a broad distribution of relaxation times. For this purpose an interpenetrating network polymer made from 25% polyurethane and 75% poly(methylmethacrylate) was chosen which does not contain water. A detailed study of this polymer will be published elsewhere (Sartor et al., 1993), but for our purpose of showing the similarity here, a set of its DSC scans for an unannealed and for variously annealed states are given in Fig. 10. It shows that, except for the temperature range of relaxation processes which obviously differ among substances, the DSC scans for the synthetic polymer in Fig. 10 have a striking resemblance with those of hydrated hemoglobin, myoglobin, and lysozyme in Figs. 3, 4, and 5. On the basis of this similarity we also conclude that the relaxation behavior, or kinetic unfreezing of the atomic or segmental motions on heating a protein, involves the same physical mechanism and phenomenology as heating a synthetic polymer.

As mentioned earlier, the main observations of this study are (i) the broad temperature range over which molecular motions gradually become active on heating and contribute to configurational entropy and heat capacity, and (ii) the appearance of an endothermic feature on annealing. The ki-

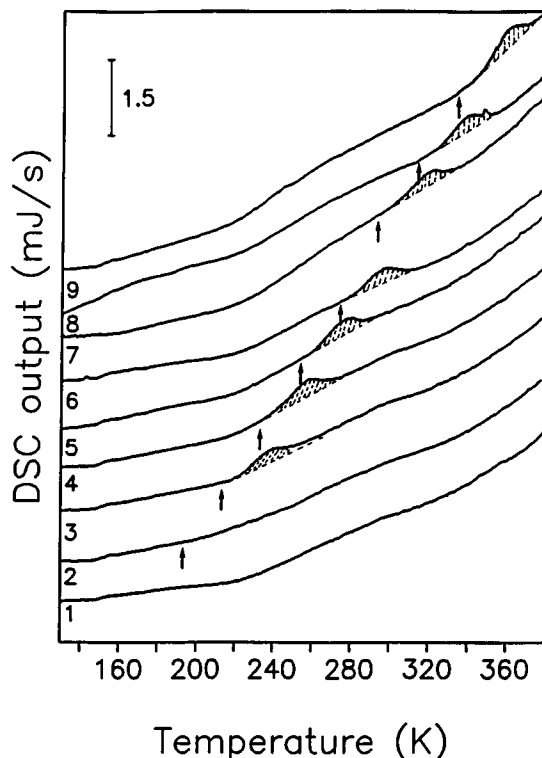


FIGURE 10 The DSC scans of an interpenetrating network polymer (25% polyurethane, 75% poly(methylmethacrylate)) heated at a rate of 30 K min^{-1} . Curve 1 is for an unannealed sample. Curves 2–9 are for the same sample but annealed at the temperature indicated by the arrow for 60 min. The procedure for annealing and for recording of the DSC scans is the same as described for the hydrated proteins in Figs. 3–5. Note the qualitative similarity with Figs. 3–5 for the three hydrated proteins (from Sartor et al., 1993).

netics of atomic and segmental motion of a protein molecule, as of polymers and molecular substances in general, which is responsible for such contributions, involves a broad distribution of relaxation times which can be represented in two ways: (1) a set of separate relaxation mechanisms for the various relaxation time components of $g(\tau)$ which represents the distribution of relaxation times, and (2) an empirical nonexponential relaxation function (DeBolt et al., 1976; Moynihan et al., 1976; Hodge and Berens, 1981, 1982). These are written as

$$\phi(t) = \int_0^{\infty} g(\tau) e^{-t/\tau} d\tau \quad (1)$$

where $\int_0^{\infty} g(\tau) d\tau = 1$ or

$$\phi(t) = \exp[-(t/\tau_0)^\beta] \quad (2)$$

where τ_0 is a characteristic time and the empirical parameter β , a measure of nonexponentiality, has a value between 0 and 1. The corresponding $g(\tau)$ is asymmetric on a $\log(\tau)$ scale, with a skew toward short times. Because of our difficulties in estimating $g(\tau)$ for very low values of β , we prefer Eq. 2. It has also been used widely in the analysis of DSC data of polymers and other glasses by several workers. We next dis-

cuss the results of our study in terms of a distribution of relaxation times described by Eq. 2.

The procedure for the analysis of the DSC data using Eq. 2 has been described frequently in the literature (DeBolt et al., 1976; Moynihan et al., 1976; Hodge and Berens, 1981, 1982) and need not be given here. Briefly,

$$\tau_0 = A \exp \left[\frac{x\Delta h^*}{RT} + \frac{(1-x)\Delta h^*}{RT_f} \right], \quad (3)$$

where A , the preexponent, is an adjustable parameter, as is x , which is a measure of the nonlinearity of the dependence of relaxation times on $\exp(1/T)$, and Δh^* is the activation enthalpy. T_f , the fictive temperature, is defined as the temperature at which the measured value of the property would be the equilibrium one. When $\beta = 1$, the relaxation occurs without distribution of times. When $x = 1$, the relaxation time follows an Arrhenius equation: this condition gives a linear equation in which τ_0 , for the relaxation of T_f , does not depend on T_f . The magnitude of A determines the characteristic relaxation time, τ_0 , for a given temperature and Δh^* determines the sensitivity of τ_0 to the temperature.

DeBolt, Moynihan, and co-workers (1976) have developed an algorithm for the calculation of DSC curves which is based on Boltzmann superposition integral and Eqs. 2 and 3. The very common combination of these equations goes back to earlier work by Mazurin et al. (1975). Annealing histories were subsequently introduced by Hodge and Berens (1981, 1982) into enthalpy relaxation calculations using these equations. This algorithm was adapted for our use, so that support for the interpretation given here can be found in the calculated or simulated DSC scans. Fig. 11 shows the simulated DSC scans using $\ln A = -135.2$, $\beta = 0.07$, $x = 0.25$, and $\Delta h^* = 300 \text{ kJ mol}^{-1}$. Curve 1 is for a sample cooled at 150 K min^{-1} from 300 K to 100 K and heated at 30 K min^{-1} . It shows a slow increase in C_p with increase in temperature. Curve 2 was obtained when the procedure included annealing at 168 K , Curve 3 for annealing at 203 K , curve 4 for annealing at 233 K , curve 5 for annealing at 253 K , and curve 6 for annealing at 278 K , all for an annealing period of 60 min at the respective temperature. It is evident that the simulated scans are in qualitative agreement with the measured DSC scans shown in Figs. 3–5. In view of the fact that quantitative fitting requires four independent and arbitrary parameters, namely A , β , x , and Δh^* , we considered that attempts at quantitative fitting would not be more revealing than the qualitative agreement already seen in Fig. 11.

Studies by other techniques (Morozov and Gevorkian, 1985; Frauenfelder and Gratton, 1986; Parak, 1986; Iben et al., 1989; Doster et al., 1986, 1989, 1990, 1991; Goldanskii and Krupyanskii, 1989; Rupley and Careri, 1991; Srajer et al., 1991; Champion, 1992; Pethig, 1992; Pissis et al., 1992) have shown onset of molecular motions in hydrated myoglobin at $\sim 180\text{--}200 \text{ K}$. This temperature is not directly comparable with our estimate of T_{\min} because the time scales of the measurements are very different. The above-mentioned studies have shown that at a given temperature mobility of the protein increases with increasing hydration.

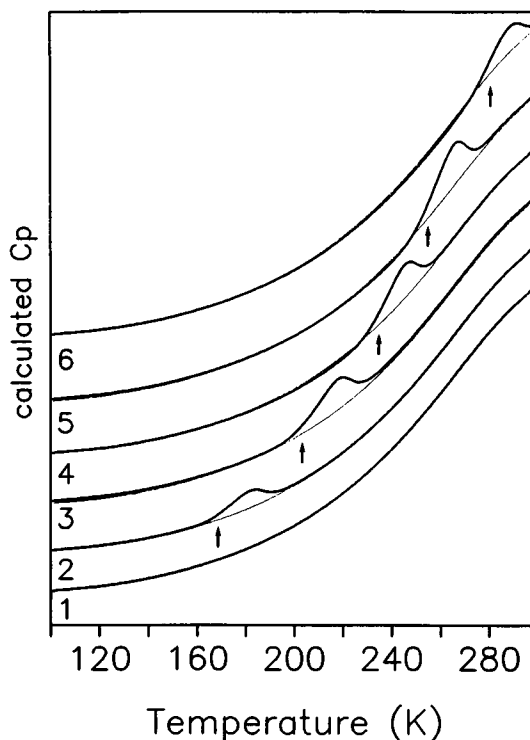


FIGURE 11 The calculated, or simulated, DSC scans showing the shape of the scan for an unannealed sample and the effect of annealing on this scan. Curve 1 is for the unannealed state and curves 2, 3, 4, 5, and 6 for the states obtained after annealing at 168 K , 203 K , 233 K , 253 K , and 278 K , respectively, all for an annealing period of 60 min . The annealing temperature is indicated by the arrows. For calculations the parameters used are: $\ln A = -135.2$, $\beta = 0.07$, $x = 0.25$, and $\Delta h^* = 300 \text{ kJ mol}^{-1}$. For simulation, the sample was cooled at 150 K min^{-1} from 300 K to 100 K , heated to the annealing temperature at 30 K min^{-1} , kept at the annealing temperature for 60 min in each case, cooled to 100 K at 30 K min^{-1} , and finally reheated to 300 K at 30 K min^{-1} when the DSC scan was calculated. Note the qualitative similarity with the experimental DSC scans for hydrated methemoglobin, metmyoglobin, and lysozyme in Figs. 3–5.

This is also apparent in our DSC study by increase of the endotherm's area with increasing hydration for the same annealing period and temperature, as shown in Figs. 7 to 9.

The DSC scans of unannealed samples shown in Fig. 1 show no discontinuity in the heat capacity contribution from molecular motions from near T_{\min} up to the denaturation region. Annealing at temperatures from 198 K to 278 K produces qualitatively similar endothermic features due to enthalpy recovery. We suggest that this is an evidence for the similarity of the underlying molecular processes at ambient and subambient temperatures, although others have cautioned that measurements taken at subambient temperatures need not necessarily be meaningful for interpreting the behavior at ambient temperature (Kuntz and Kauzmann, 1974; Rupley and Careri, 1991).

CONCLUSIONS

The kinetic unfreezing of atomic and segmental motions of hemoglobin, myoglobin, and lysozyme which is caused by

the presence of water H-bonded to its atoms, occurs over a temperature range extending from ≈ 150 K up to the denaturation temperature. This is a reflection of the presence of a large number of local structures in which atomic and molecular segments diffuse at different time scales at a fixed temperature. For a given temperature, those molecular motions with a relaxation time of less than ~ 10 s contribute to the heat capacity in a DSC scan made by heating at 30 K min^{-1} . As the temperature is increased, the number of atomic and segmental motions with a relaxation time less than ~ 10 s increases. This contributes to the configurational enthalpy and entropy and C_p increases slowly without showing an abrupt increase characteristic of the glass \rightarrow liquid transition.

Annealing at different temperatures from 198 K to 278 K causes enthalpy relaxation of those local structures whose relaxation times are less than or the order of the annealing time. Rate heating of the annealed sample shows an endothermic effect (or region in the DSC scan) which resembles the C_p overshoot in the usually observed glass \rightarrow liquid transition. This interpretation is confirmed by measurement on a synthetic polymer which has a broad distribution of relaxation times and by simulation of DSC scans, where similarly featureless DSC scans are observed for unannealed samples and annealing causes an analogous effect. Further analysis suggests that the lower limit of relaxation time corresponds to the motions of $>\text{N}-\text{H}$ and $-\text{O}-\text{H}$ groups.

Note added in proof

Recently Miyazaki et al. (1993. *Chem. Phys. Lett.* 213:303–308) reported calorimetric evidence for intense sharp glass transitions in myoglobin crystals, with T_g value at 188 and 216 K. This is in conflict with our observations in this study and with those of Doster et al. (1986). We give an alternative interpretation of their observations as follows. Miyazaki et al. (1993) also reported that their myoglobin samples contained in the dried crystal 21.8 wt% NaH_2PO_4 and 27.0 wt% K_2HPO_4 . Van den Berg and Rose (1959. *Archiv. Biochem. Biophys.* 81:319–329) first reported that in a freeze-concentrated solution of sodium phosphate containing buffers the $\text{NaH}_2\text{PO}_4/\text{Na}_2\text{HPO}_4$ molar ratio approaches a value of ~ 57 because the acidic buffer component does not crystallize but forms a highly concentrated aqueous solution. Such a solution is expected to show an intense T_g . We have investigated by DSC an aqueous solution of the buffer composition reported by Miyazaki et al. (1993) and observed both on cooling and heating intense changes in heat capacity which were in the same temperature region as reported by Miyazaki et al. (1993) for their T_g values for myoglobin. These should help to prevent misconceptions that could arise from this conflict.

We are grateful for financial support by the Forschungsförderungsfonds of Austria (project P9175-PHY) and to Dr. W. Doster for discussions and for reading the manuscript.

REFERENCES

- Angell, C. A., and L. M. Torrell. 1983. Short time structural relaxation processes in liquids: comparison of experimental and computer simulation glass transitions on picosecond time scales. *J. Chem. Phys.* 78: 937–945.
- Avramova, N., and S. Fakirov. 1983. On the determination of the equilibrium melting temperature of nylon 66 and nylon 12. *Polymer Commun.* 24:19–21.
- Berens, A. R. and I. M. Hodge. 1982. Effects of annealing and prior history on enthalpy relaxation in glassy polymers. I. Experimental study of poly(vinyl chloride). *Macromolecules.* 15:756–761.
- Champion, P. M. 1992. Raman and kinetic studies of myoglobin structure and dynamics. *J. Raman Spectrosc.* 23:557–567.
- Cooke, R., and I. D. Kuntz. 1974. The properties of water in biological systems. *Annu. Rev. Biophys. Bioeng.* 3:95–125.
- DeBolt, M. A., A. J. Easteal, P. B. Macedo, and C. T. Moynihan. 1976. Analysis of structural relaxation in glass using rate heating data. *J. Am. Ceram. Soc.* 59:16–21.
- Doster, W., A. Bachleitner, R. Dunau, M. Hiebl, and E. Lüscher. 1986. Thermal properties of water in myoglobin crystals and solutions at sub-zero temperatures. *Biophys. J.* 50:213–219.
- Doster, W., S. Cusack, and W. Petry. 1989. Dynamical transition of myoglobin revealed by inelastic neutron scattering. *Nature (Lond.)*. 337:754–756.
- Doster, W., S. Cusack, and W. Petry. 1990. Dynamic instability of liquidlike motions in a globular protein observed by inelastic neutron scattering. *Phys. Rev. Lett.* 65:1080–1084.
- Doster, W., S. Cusack, and W. Petry. 1991. Structural dynamics of proteins, scaling behaviour and liquid glass transition. *J. Non-Crystall. Solids.* 131: 133:357–361.
- Franks, F., and R. H. M. Hatley. 1985. Low temperature unfolding of chymotrypsinogen. *Cryo Lett.* 6:171–180.
- Franks, F., R. H. M. Hatley, and H. L. Friedman. 1988. The thermodynamics of protein stability: cold destabilization as a general phenomenon. *Biophys. Chem.* 31:307–315.
- Fransson, A., and G. Bäckström. 1987. Isothermal enthalpy relaxation of glycerol. *Int. J. Thermophys.* 8:351–362.
- Frauenfelder, H., and E. Gratton. 1986. Protein dynamics and hydration. *Methods Enzymol.* 127:207–216.
- Goldanskii, V. I., and Y. F. Krupyanskii. 1989. Protein and protein-bound water dynamics studied by Rayleigh scattering of Mössbauer radiation. *Q. Rev. Biophys.* 22:39–92.
- Hallbrucker, A., Mayer, E., and Johari, G. P. 1989. The heat capacity and glass transition of hyperquenched glassy water. *Philos. Mag.* 60B: 179–187.
- Hodge, I. M., and Berens, A. R. 1982. Effects of annealing and prior history on enthalpy relaxation in glassy polymers. 2. Mathematical modeling. *Macromolecules* 15:762–770.
- Hofer, K., E. Mayer, and G. P. Johari. 1990. Glass-liquid transition of water and ethylene glycol solution in poly(2-hydroxyethyl methacrylate) hydrogel. *J. Phys. Chem.* 94:2689–2696.
- Iben, I. E. T., D. Braunstein, W. Doster, H. Frauenfelder, M. K. Hong, J. B. Johnson, S. Luck, P. Ormos, A. Schulte, P. C. Steinbach, A. H. Xie, and R. D. Young. 1989. Glassy behavior of a protein. *Phys. Rev. Lett.* 62:1916–1919.
- Johari, G. P., A. Hallbrucker, and E. Mayer. 1987. The glass transition of hyperquenched water. *Nature (Lond.)*. 330:552–553.
- Kuntz, I. D., and W. Kauzmann. 1974. Hydration of proteins and polypeptides. *Adv. Protein Chem.* 28:239–345.
- Mazurin, O. V., S. M. Rekhson, and Yu. K. Startsev. 1975. Role of viscosity in calculating relaxation of the properties of a glass in the vitrification interval. *Fiziol. Khim. Stekla* 1:438–442.
- Morozov, V. N., and S. G. Gevorkian. 1985. Low-temperature glass transition in proteins. *Biopolymers* 24:1785–1799.
- Moynihan, C. T., P. B. Macedo, C. J. Montrose, P. K. Gupta, M. A. DeBolt, J. F. Dill, B. E. Dom, P. W. Drake, A. J. Easteal, P. B. Elterman, R. P. Moeller, H. Sasabe, and J. A. Wilder. 1976. Structural relaxation in vitreous materials. *Ann. N.Y. Acad. Sci.* 279:15–36.
- Parak, F. 1986. Correlation of protein dynamics with water mobility: Mössbauer spectroscopy and microwave absorption methods. *Methods Enzymol.* 127:196–206.
- Pethig, R. 1992. Protein-water interactions determined by dielectric methods. *Annu. Rev. Phys. Chem.* 43:177–205.
- Pissis, P., A. Anagnostopoulou-Konsta, L. Apeki, D. Daoukaki-Diamanti, and C. Christodoulides. 1992. Dielectric studies on glass transitions in biological systems. *IEEE Trans. Electr. Insulation.* 27:820–825.
- Poole, P. L., and J. L. Finney. 1986. Solid-phase protein hydration studies. *Methods Enzymol.* 127:284–293.

- Privalov, P. L., Yu. V. Griko, S. Yu. Venyaminov, and V. P. Kutysenko. 1986. Cold denaturation of myoglobin. *J. Mol. Biol.* 190:487-498.
- Rothgeb, T. M., and F. R. N. Gurd. 1978. Physical methods for the study of myoglobin. *Methods Enzymol.* 52:473-486.
- Rupley, J. A., and G. Careri. 1991. Protein hydration and function. *Adv. Protein Chem.* 41:37-172.
- Sartor, G., A. Hallbrucker, K. Hofer, and E. Mayer. 1992. Calorimetric glass-liquid transition and crystallization behavior of a vitreous, but freezable, water fraction in hydrated methemoglobin. *J. Phys. Chem.* 96: 5133-5138.
- Sartor, G., E. Mayer, and G. P. Johari. 1993. Thermal history and enthalpy relaxation of an interpenetrating network polymer with exceptionally broad relaxation time distribution. *J. Polymer Sci.* In press.
- Srajer, V., L. Reinisch, and P. M. Champion. 1991. Investigation of laser-induced long-lived states of photolyzed MbCO. *Biochemistry.* 30: 4886-4893.
- Waterman, M. R. 1978. Spectral characterization of human hemoglobin and its derivatives. *Methods Enzymol.* 52:456-463.
- Wunderlich, B. 1990. Thermal Analysis. Academic Press, Boston. 186-202.